Hemato-vascular specification requires *arnt1* and *arnt2* genes in zebrafish embryos

Authors: Hailey E. Edwards, Jaclyn P. Souder, Daniel A. Gorelick

Center for Precision Environmental Health, Department of Molecular and Cellular Biology, Baylor College of Medicine, Houston, Texas, USA

Correspondance to DAG gorelick@bcm.edu

ABSTRACT

During embryonic development, a subset of cells in the mesoderm germ layer are specified as hemato-vascular progenitor cells, which then differentiate into endothelial cells and hematopoietic stem and progenitor cells. In zebrafish, the transcription factor *npas4l*, also known as *cloche*, is required for the specification of hemato-vascular progenitor cells. However, it is unclear if *npas4l* is the sole factor at the top of the hemato-vascular specification cascade. Here we show that *arnt1* and *arnt2* genes are required for hemato-vascular specification. We found that *arnt1;arnt2* double homozygous mutant zebrafish embryos (herein called *arnt1/2* mutants), but not *arnt1* or *arnt2* single mutants, lack blood cells and most vascular endothelial cells. *arnt1/2* mutants have reduced or absent expression of *etv2* and *tal1*, the earliest known endothelial and hematopoietic transcription factor genes. *npas4l* and *arnt* genes are PAS domain-containing bHLH transcription factors that function as dimers. We found that Npas4l binds both Arnt1 and Arnt2 proteins *in vitro*, consistent with the idea that PAS domain-containing bHLH transcription factors act in a multimeric complex to regulate gene expression. Our results demonstrate that *npas4l*, *arnt1* and *arnt2* act together as master regulators of endothelial and hematopoietic cell fate. Our results also demonstrate that *arnt1*

and *arnt2* act redundantly in a transcriptional complex containing *npas4l*, but do not act redundantly when interacting with another PAS domain-containing bHLH transcription factor, the aryl hydrocarbon receptor. Altogether, our data enhance our understanding of hemato-vascular specification and the function of PAS domain-containing bHLH transcription factors.

INTRODUCTION

Endothelial and hematopoietic cells are derived from the mesoderm during vertebrate embryogenesis. These two cell types are closely linked and arise from a common progenitor during development (Huber et al., 2004; Kataoka et al., 2011; Liao et al., 2000). The differentiation and specification of endothelial and hematopoietic cells occurs in two waves—primitive and definitive hematopoiesis (Costa et al., 2012; Paik and Zon, 2010; Palis et al., 1999). During primitive hematopoiesis the first hemato-vascular progenitors are observed in the lateral plate mesoderm of zebrafish and in the extraembryonic yolk sac mesoderm of mice (Lee et al., 1994; Palis et al., 1999; Stainier et al., 1993). These progenitors give rise to blood islands which contain primitive erythroid cells (Palis et al., 1999). During definitive hematopoiesis in mice and zebrafish, fully multipotent hematopoietic stem cells (HSCs) are derived from specialized epithelial cells, hemogenic endothelium (Hirschi, 2012; Kobayashi et al., 2014).

In humans, the genes that drive the specification of hemato-vascular progenitors from the multipotent mesoderm are not completely understood. We have a more complete understanding of this process in other vertebrates. In zebrafish and chicken, Neuronal PAS 4-like (*npas4l)* is essential for the specification of hemato-vascular progenitors from multipotent mesoderm (Reischauer et al., 2016; Weng et al., 2020). Mammals do not appear to have a

47 *npas4l* homolog in their genomes and the mammalian functional equivalent to zebrafish *npas4l*
48 is unknown. Many genes involved in embryonic hematopoiesis are conserved between
49 zebrafish, mice, and humans (Aplan et al., 1992; Brownlie et al., 1998; Casie Chetty et al.,
50 2017; Dooley et al., 2005; Ferrara et al., 1996; Gong et al., 2004; Kalev-Zylinska et al., 2002b;
51 Kataoka et al., 2011; Okuda et al., 1996; Wang et al., 1996), but *npas4l* appears to be an
52 exception. Understanding the specific mechanisms of hemato-vascular specification in
53 zebrafish may help identify functional homologs in humans and other mammals.
54 Understanding the specific mechanisms of hemato-vascular specification may prove useful in
55 regenerative therapies for blood and vascular diseases. Recipients of embryonic stem cell-
56 based regenerative therapies have an increased risk of tumor formation. A promising
57 alternative, which ameliorates the risk of tumor formation, is to produce specific multipotent
58 progenitors from embryonic stem cells prior to transplantation (Doss et al., 2012; Gunaseeli et
59 al., 2010).
60 Zebrafish embryos and larvae are an ideal organism in which to study hemato-vascular
61 development *in vivo*. Zebrafish oocytes are fertilized externally and embryos are optically
62 transparent. Zebrafish embryos can survive up to 7 days post fertilization without circulating
63 red blood cells because oxygen can freely diffuse through the skin (Hughes et al., 2019;
64 Pelster and Burggren, 1996). This trait allows for characterization of cardiovascular
65 phenotypes that would be lethal in embryos from other organisms.
66 In zebrafish, endothelial cells and HSCs can be derived from a single hemato-vascular
67 progenitor cell population called the hemangioblast, which is hypothesized to exist in mammals
68 but has not been definitively confirmed (Huber et al., 2004; Moore et al., 2018; Shu et al.,
69 2015; Zhang and Featherstone, 2020). It has been previously reported that the basic helix-

70 loop-helix Per-Arnt-Sim (bHLH-PAS) transcription factor, *npas4l,* is the master regulator of
71 hemato-vascular specification in zebrafish (Reischauer et al., 2016) and in chicken (Weng et
72 al., 2020).

73 bHLH-PAS transcription factors are classified as Class I or Class II, which must
74 dimerize to regulate transcription (Erbel et al., 2003; Pongratz et al., 1998)(Figure 1A). Npas4l
75 is a Class I bHLH-PAS protein, but its binding partner during hemato-vascular progenitor
76 specification is not known. We hypothesized that Arnt1 or Arnt2 is the dimerization partner of
77 Npas4l in zebrafish because there are only 4 bHLH-PAS Class II proteins encoded in the
78 zebrafish genome and *arnt1* and *arnt2* genes are expressed at the the same stages of embryo
79 development as *npas4l* (Prasch et al., 2006; Reischauer et al., 2016; Tanguay et al., 2000).

80 To test this hypothesis, we examined hemato-vascular development in zebrafish with
81 loss-of-function mutations in *arnt1* and *arnt2* genes. We find that Arnt1 and Arnt2 are essential
82 for hemato-vascular specification. Double homozygous *arnt1;arnt2* zebrafish embryos
83 phenocopy *npas4l* mutants (also called *cloche*), showing lack of circulating blood, absence of
84 hematopoietic stem and progenitor cells, and dramatic reduction in the number of vascular
85 endothelial cells. Additionally, we show that zebrafish Npas4l protein interacts with both
86 zebrafish Arnt1 and zebrafish Arnt2 proteins *in vitro*. Together, our results suggest that Arnt1
87 and Arnt2 act redundantly and form a transcriptional complex with Npas4l that sits atop the
88 hemato-vascular specification cascade.

89

90 **MATERIALS AND METHODS**
91

92 **Zebrafish**

93 Adult zebrafish were raised at 28.5°C on a 14-h light, 10-h dark cycle in the UAB Zebrafish
94 Research Facility or the BCM Zebrafish Research Facility in an Aquaneering recirculating
95 water system (Aquaneering, Inc., San Diego, CA) and a Tecniplast recirculating water system
96 (Tecniplast USA, Inc., West Chester, PA). All zebrafish used for experiments were wild-type
97 AB strain (Westerfield, 2000) and all mutant lines were generated on the AB strain. All
98 procedures were performed in accordance with Institutional Animal Care and Use Committees
99 (IACUC) and BCM guidelines.
100

101 **Embryo collection**

102 Adult zebrafish were allowed to spawn naturally in pairs or in groups. Embryos were collected
103 in intervals of 20 minutes to ensure precise developmental timing or staged following
104 collection, placed in 60 cm^2 Petri dishes at a density of no more than 100 per dish in E3B
105 media (60X E3B: 17.2g NaCl, 0.76g KCl, 2.9g $CaCl_2$-$2H_2O$, 2.39g $MgSO_4$ dissolved in 1L Milli-
106 Q water; diluted to 1X in 9L Milli-Q water plus 100 µL 0.02% methylene blue), and then stored
107 in an incubator at 28.5°C on a 14-h light, 10-h dark cycle.
108

109 **Genotyping adult zebrafish**

110 Genomic DNA was isolated from tail biopsies from individual adult zebrafish by incubation in
111 50 µL ELB (10 mM Tris pH 8.3, 50 mM KCl, 0.3% Tween 20) with 0.5 µL proteinase K (800
112 U/ml, NEB) in 96 well plates, one sample per well, at 55°C for 8 hours (tail biopsies).
113 Proteinase K was inactivated by incubation at 98°C for 10 minutes and DNA was stored at -
114 20°C. Genotyping was performed by PCR and high-resolution melting curve analysis as
115 described (Parant et al., 2009; Romano et al., 2017). All melting curves were generated with a

116 Bio-Rad CFX96 Real-Time System over a 70-95°C range and analyzed with the Bio-Rad CFX
117 Manager 3.1 or the Bio-Rad CFX Maestro 4.1 software. All mutations were confirmed by TA
118 cloning and sequencing.
119
120 **CRISPR-Cas9 Mutant Generation**
121 Cas9 mRNA and gRNAs for *arnt1,* and *arnt2* mutants were generated as previously described
122 (Romano et al., 2017; Souder and Gorelick, 2019). Cas9 mRNA was transcribed from a
123 linearized pT3TS-nCas9n plasmid, Addgene #46757 (Jao et al., 2013), and purified. The target
124 sequences were identified using CHOPCHOP (Labun et al., 2016; Labun et al., 2019).
125 Oligonucleotides were annealed to each other and cloned into a pT7-gRNA plasmid, Addgene
126 #46759 (Jao et al., 2013). Oligonucleotides utilized are shown in Table 1. gRNAs were
127 synthesized from plasmids using a MEGAshortscript T7 Transcription Kit (Invitrogen AM1354)
128 and purified.
129 One-cell-stage embryos were injected using glass needles pulled on a Sutter
130 Instruments Fleming/Brown Micropipette Puller, model P-97 and a regulated air-pressure
131 micro-injector (Harvard Apparatus, NY, PL1–90). Each embryo was injected with a 1nL
132 solution containing one gRNA for *arnt1* and one gRNA for *arnt2* (30 ng/μL per target), Cas9
133 mRNA (150 ng/μL), and 0.1% phenol red. Mixtures were injected into the yolk of each embryo.
134 Approximately, 100 injected embryos per gRNA pair were raised to adulthood and crossed to
135 AB zebrafish to generate F1 embryos. F1 offspring with heritable mutations were sequenced to
136 identify mutations predicted to cause loss of function.
137
138 **Live Imaging**

139 Embryos were imaged with a Nikon SMZ25 microscope equipped with a Hamamatsu ORCA-
140 Flash4.0 digital CMOS camera. Images were equally adjusted for brightness and contrast in
141 Adobe Photoshop CC 2020. Embryos and larvae were anesthetized with 0.04% tricaine and
142 imaged in Petri dish containing E3B. All embryos were genotyped after imaging.
143

144 **Whole mount *in situ* hybridization**

145 *etv2, tal1, runx1,* and *flk1* antisense RNA probes were used as described (Moore et al., 2013;
146 Thisse and Thisse, 2008). All DNA clones were verified by sequencing. Digoxigenin-labeled
147 antisense RNA probes were synthesized using T7 for *runx1* and *flk1*, or T3 for *etv2*.
148 Colorimetric *in situ* hybridization (ISH) was performed on fixed zebrafish embryos and larvae
149 as previously described, with 5% dextran in the hybridization buffer (Lauter et al., 2011; Thisse
150 and Thisse, 2008). Following ISH, embryos were washed several times in 1x PBST
151 (phosphate buffered saline, 0.01% Tween), cleared with glycerol or mounted in 3%
152 methylcellulose on a class coverslip, and imaged on either a Nikon SMZ18 stereoscopic
153 microscope or an inverted Nikon ECLIPSE Ti2-E microscope. Embryos were then genotyped.
154 Genomic DNA was extracted using the HotSHOT protocol (Dobrzycki et al., 2018). Briefly,
155 embryos were suspended in 20 µL of lysis buffer (25 mM NaOH, 0.2 mM EDTA) and incubated
156 at 95°C for 30 minutes, cooled to 4°C, then an equal volume of neutralization buffer (40 mM
157 Tris-HCl) was added. DNA regions of interest were amplified with JumpStart REDTaq
158 ReadyMix (Sigma-Milipore, P0982) PCR according to manufacturer's protocols.
159

160 **Cell Culture and Transient Transfection**

161 HEK293T cells (gift of Dr. Charles Foulds), were thawed and maintained at 37°C in humidified
162 5% CO_2 atmosphere incubator. Cells were cultured in DMEM supplemented with 10% fetal
163 bovine serum (FBS) (Gibco, 2062564), and 1% penicillin-streptomycin (Gibco, 15140-122).
164 After 24 hours passaging in a 100mm plate at a density of 2.2 x 10^6 cells per dish and reaching
165 at least 70 confluency, the media was changed to DMEM supplemented with 1% dialyzed
166 FBS. Cells were transiently transfected with 12 µg of total DNA and Lipofectamine 2000
167 according to manufacturer's instructions (Invitrogen, 2400439) with *npas4l-v5* together with
168 either *arnt1-myc* or *arnt2-HA* plasmid DNA.
169 Cloning of plasmids for expression in cultured cells was performed as follows. For
170 npas4l-V5, we took pCS2+npas4lORF (gift of Dr. Leonard Zon) that contains the open reading
171 frame (ORF) of zebrafish *npas4l* downstream of the CMV promoter. This plasmid was modified
172 to include a C-terminal V5 tag using Q5 Site-Directed Mutagenesis Kit (New England Biolabs,
173 #E0554S). For arnt1-myc, we synthesized a plasmid containing CMV promoter driving a
174 codon-optimized zebrafish *arnt1* ORF (ENSDART00000081852.5) with a C-terminal myc tag
175 (Twist Bioscience, San Francisco, CA). For arnt2-myc, we synthesized a gene block of the
176 zebrafish *arnt2* ORF (ENSDART00000158162.2, Integrated DNA Technologies). The gene
177 block was integrated into a plasmid containing a CMV promoter using pcDNA3.3-TOPO TA
178 cloning kit (Invitrogen, K8300-01) in accordance with manufacturer's instructions. A C-terminal
179 HA tag was added using Q5 Site-Directed Mutagenesis Kit (New England Biolabs, #E0554S).
180

181 **Co-immunoprecipitation and Western blot**

182 Transiently transfected cells were washed with ice cold PBS and lysed in 500 µL of 1x RIPA
183 buffer containing Pierce Protease (ThermoScientific, A32955). Cells were sonicated in 6 x 30

184 second intervals using a Bioruptor 300 Machine (Diagenode), then centrifuged for 10 minutes
185 at 10,000g at 4°C. The lysate (supernatant) was removed from the pellet and placed in fresh
186 1.5mL Eppendorf tube. Cell lysate was precleared with Protein A beads (Invitrogen #159 18-
187 014) for 30 minutes 4°C, incubated with either 5 µg of V5 antibody (ThermoFisher Scientific
188 R960-25) or myc antibody (SantaCruz, SC-40) diluted 1:200 for 1 hour, then
189 immunoprecipitated with 20 µL of Protein A beads for 1 hour at 4°C. The beads were washed
190 three times with RIPA buffer and once with PBS and finally suspended in 30µL of PBS. Equal
191 volume of 2x Laemmli Sample Buffer (BioRad, cat# 1610737) was added to each sample and
192 boiled for 5 minutes at 95°C then placed on ice. Samples were run on 4-20% Mini-PROTEAN
193 TGX gels (BioRad, cat# 4561093) and transferred onto PVDF membrane using Trans-Blot
194 Turbo Transfer System (BioRad) using the pre-defined Mixed MW program. The membranes
195 were washed several times with 1x Tris-Buffered Saline, 0.1% Tween 20 (TBST)
196 (GBiosciences, R043) and incubated for 1 hour with agitation in 5% milk in 1x TBST.
197 Membranes were probed with 1:1000 V5-HRP (ThermoFisher Scientific, R960-25), 1:1000
198 myc-HRP (SantaCruz, SC-40), or 1:200 HA (Cell Signaling, 3724) antibodies rocking overnight
199 at 4°C. Membranes were washed 5 times with 1xTBST on orbital rocker for 15 minutes at room
200 temperature. Membranes probed with the anti-HA antibody were then probed with 1:10,000
201 IRDye 800CW donkey anti-rabbit (Licor, 926-32213) in 2.5%-5% milk in 1x TBST for 1 hour
202 and then washed multiple times with 1xTBST on orbital rocker for 5 minutes prior to imaging.
203 Membranes probed with HRP conjugated antibodies were developed using Clarity™ Western
204 ECL Substrate (BioRad, 170-5061). Membranes were imaged using BioRad ChemiDoc™ MP
205 Imaging System.
206

207 **TCDD exposure**

208 At 1-day post fertilization (dpf) embryos were exposed to 10 ng/mL 2,3,7,8-
209 tetrachlorodibenzodioxin (TCDD, AccuStandard Inc, D404N) or vehicle (0.1% DMSO). All
210 treatments were performed on a single clutch of at least 20 embryos; embryos treated with
211 vehicle were from the same clutches as embryos treated with TCDD. Chemical exposures
212 were performed on at least 2 clutches per genotype. Embryos were raised at 28.5°C on a 14-h
213 light, 10-h dark cycle until 3 dpf, when they were imaged and then genotyped.

214

215

RESULTS

arnt1/2 homozygous mutants lack circulating blood

To determine if *arnt1* or *arnt2* is required for hemato-vascular development, we generated heritable mutant alleles for *arnt1 (arnt1^{bcm1}* and *arnt1^{bcm2})* and *arnt2 (arnt2^{bcm3})* using CRISPR/Cas9. For *arnt1^{bcm1},* we generated zebrafish with a 5 bp insertion in exon 5, which results in a frameshift at amino acid (AA) 126 and a premature stop codon in the first PAS domain at AA139 (Fig. 1B). For *arnt1^{bcm2}*, we generated zebrafish with an 11 bp deletion in exon 10, which results in a frameshift at AA230 and a premature stop codon between the two PAS domains at AA250 (Fig. 1B). We did not observe any phenotypic differences between homozygous *arnt1$^{bcm/bcm1}$ and arnt1$^{bcm2/bcm2}$* mutant embryos. These mutants are morphologically indistinct from wildtype during development and homozygous adults are viable and fertile, which is consistent with previously published *arnt1* mutants (Marchi et al., 2020). We also generated maternal zygotic *arnt1* mutants (derived from homozygous *bcm1* or *bcm2* parents) and these were morphologically indistinct from wildtype. For *arnt2^{bcm3},* we generated zebrafish with a 3 bp deletion and 1 bp insertion in exon 9, which resulted in a missense mutation at AA286 and a premature stop codon between the two PAS domains at AA287 (Fig. 1C). Homozygous *arnt2* mutants *(arnt2$^{bcm3/bcm3}$*) were viable at 5 days post fertilization (dpf) and grossly morphologically normal, however they did not survive to adulthood. Our observations are consistent with independently generated *arnt2* mutant zebrafish lines (Hill et al., 2009; Lohr et al., 2009).

We crossed *arnt1$^{bcm2/+}$; arnt2$^{bcm3/+}$* adult fish to each other and analyzed the phenotype and genotype of the resulting embryos. We observed all genotypes at the expected Mendelian ratios (**Table 1**). The single mutant larvae, *arnt1$^{bcm2/bcm2}$*, herein called *arnt1* mutants (**Fig. 1D and D'**), and *arnt2$^{bcm3/bcm3}$*, herein called *arnt2* mutants (**Fig. 1E and E'**), are phenotypically indistinguishable from their wildtype siblings by gross morphology (**Fig. 1C and C'**). However, *arnt1$^{bcm2/bcm2}$;arnt2$^{bcm3/bcm3}$* larvae, herein called *arnt1/2* mutants, showed a clear phenotype (**Fig. 1F**). These larvae lack all circulating blood (**Fig. 1H , M3 and M4**). All other intermediate *arnt1;arnt2* genotypes, e.g.,

241 *arnt1*$^{bcm2/+}$*;arnt2*$^{bcm3/bcm3}$, appeared phenotypically wildtype (Fig. 1G, and data not shown). These results
242 suggest that *arnt1* and *arnt2* function redundantly, because only the *arnt1/2* double homozygous
243 mutants show a phenotype. Additionally, the *arnt1/2* mutant phenotype appears identical to the
244 previously described *npas4l* mutant phenotype (also known as *cloche*) (Reischauer et al., 2016;
245 Stainier et al., 1995a). Like *npas4l* mutants, *arnt1/2* mutants exhibit cardiac edema with enlarged heart
246 atrium, likely a secondary effect of the lack of blood and endocardial cells (Fig 1G). Taken together,
247 these data suggest that *arnt1* and *arnt2* have a similar function as *npas4l*.
248

249 ***arnt1/2* mutants have reduced expression of hematopoietic and endothelial cell markers at 2 dpf**

250 We hypothesized that the Arnt proteins are dimerization partners with Npas4l and that *arnt1/2*
251 mutants would exhibit the same phenotypes as *npas4l* mutants. Therefore, we examined *arnt1/2*
252 mutant embryos for additional phenotypes found in *npas4l* mutants. Previous studies determined that
253 *npas4l* mutants lack almost all endothelial cells, except some cells located in the lower trunk and caudal
254 tail of the larvae (Liao et al., 1997; Stainier et al., 1995a). To determine if our *arnt1/2* mutants showed a
255 similar reduction in endothelial cells, we performed whole-mount *in situ* hybridization (WISH) on 2 dpf
256 embryos for *flk-1* (also known as *kdrl)*. *flk-1*, a widely used marker of endothelial cells in blood vessels,
257 is essential for the development of blood vessels in mice and zebrafish (Dumont et al., 1995; Liao et al.,
258 1997; Shalaby et al., 1995). We found that *maternal zygotic arnt1* mutants (*MZarnt1*) and *arnt2*
259 mutants showed clear expression of *flk-1* in the vasculature, similar to wild type (**Fig 2B-C)**. In contrast,
260 *arnt1/2* mutants had a reduced number of *flk-1*-positive cells (**Fig. 2D and D'**). The *flk-1*-positive cells
261 present in the *arnt1/2* mutant were in the caudal tail and likely comprised a portion of the caudal vein
262 (**Fig. 2D'**), similar to the *flk-1* expression pattern seen in *npas4l* mutants (Liao et al., 1997). This
263 suggests that *npas4l* and *arnt1* or *arnt2* are required for the development of most blood vessels.

264 In addition to a significant reduction of endothelial cells, *npas4l* mutants show a reduction in the
265 number of hematopoietic stem cells (HSC) (Stainier et al., 1995a; Thompson et al., 1998). To

266 determine if *arnt1/2* mutants contain HSCs, we examined *runx1* expression by WISH. *runx1* is a marker
267 of HSCs and is required for definitive hematopoiesis in zebrafish (Kalev-Zylinska et al., 2002a). By 48
268 hpf, *runx1*-positive HSCs are localized to the area between the dorsal aorta and the posterior caudal
269 vein (Lam et al., 2009). At 2 dpf, wildtype**,** *arnt1*, and *arnt2* single mutants all contain *runx1*-positive
270 cells in the blood island region (**Fig 2E-G)**, indicating the presence of HSCs. However, *arnt1/2* mutants
271 lack *runx1*-positive cells in this region (**Fig. 2H**). This suggests that *arnt1* or *arnt2* is necessary for
272 hematopoietic cell development during embryogenesis, similar to *npas4l* (Liao et al., 1998; Stainier et
273 al., 1995a; Thompson et al., 1998).
274
275 **Hematopoietic and endothelial progenitor populations are reduced in *arnt1/2* mutants**
276 Hematopoietic cells and endothelial cells arise from a common progenitor population in
277 zebrafish (Vogeli et al., 2006). To determine if *arnt1/2* mutants have a reduction of hemato-vascular
278 progenitor cells, we performed WISH on embryos at the 4-6 somite stage and examined expression of
279 the earliest known regulators of endothelial and hematopoietic cell differentiation: *etv2* and *tal1,* both of
280 which are expressed in the posterior lateral plate mesoderm (PLPM) during early somitogenesis stages
281 (Qian et al., 2005; Reischauer et al., 2016; Stainier et al., 1995a; Thompson et al., 1998). We bred
282 *arnt1*$^{bcm2/+}$*; arnt2*$^{bcm3/+}$ adults to each other to generate *arnt1/2* mutant, *arnt1* mutant, *arnt2* mutant, and
283 wildtype embryos. We then performed WISH to examine the expression of *etv2* (**Fig. 3A and B**, n=516
284 embryos from 5 clutches) or *tal1* (**Fig. 3C and D**, n=665 embryos from 3 clutches). 8% and 6% of
285 embryos showed reduced expression of *etv2* and *tal1*, respectively, neither of which is statistically
286 significantly different from the expected Mendelian ratio of 6.25% double homozygous mutant embryos
287 (binomial test, *etv2* n=516 $p>0.05$; *tal1* n=665 $p>0.05$). To confirm that the observed reduction of *etv2*
288 and *tal1* in these embryos correlates with the *arnt1/2* double homozygous mutant genotype, following
289 WISH we genotyped 24 of the embryos with absent or reduced expression of *etv2* and 17 with absent
290 or reduced expression of *tal1*. 100% of the low/no expressing *etv2* embryos were *arnt1/2* double

291 homozygous mutants, while 83% of the low/no expressing *tal1* embryos were *arnt1/2* double
292 homozygous mutants, demonstrating a strong correlation between the reduced expression of *etv2* and
293 *tal1* and the *arnt1/2* double homozygous genotype. Additionally, we genotyped 26 of the embryos with
294 normal expression of *etv2* and 7 with normal expression of *tal1.* 7.7% of the normal expressing *etv2*
295 embryos were *arnt1/2* mutants (genotypes of the 26 embryos: 2 *arnt1/2* mutants, 1 wildtype, 3
296 *arnt1*$^{bcm2/bcm2}$, 4 *arnt1*$^{bcm2/bcm2}$;*arnt2*$^{bcm3/+}$, 4 *arnt1*$^{bcm2/+}$, 5 *arnt1*$^{bcm2/+}$;*arnt2*$^{bcm3/+}$, 4 *arnt1*$^{bcm2/+}$;*arnt2*$^{bcm3/bcm3}$,
297 1 *arnt2*$^{bcm3/bcm3}$, and 3 *arnt2*$^{bcm3/+}$), while 0% of the normal expressing *tal1* embryos were *arnt1/2*
298 mutants (genotypes of the 7 embryos: 1 *arnt1*$^{bcm2/+}$;*arnt2*$^{bcm3/+}$, 1 *arnt1*$^{bcm2/+}$;*arnt2*^{bcm3bcm3}, 1 *arnt1*$^{bcm2/+}$, 1
299 *arnt2*$^{bcm3/+}$, and 3 *arnt1*$^{bcm2/bcm2}$;*arnt2*$^{bcm3/+}$). We conclude that *arnt1* and *arnt2* are required for hemato-
300 vascular progenitor specification. Previous findings demonstrated that *npas4l* is a master regulator of
301 hemato-vascular progenitor specification (Reischauer et al., 2016). Together, these results demonstrate
302 that *npas4l*, *arnt1* and *arnt2* are co-master regulators of hemato-vascular specification.
303

304 **Npas4l interacts with both Arnt1 and Arnt2**

305 Npas4l is a Class I bHLH-PAS domain transcription factor (Reischauer et al., 2016), and as
306 such, must heterodimerize with Class II bHLH-PAS transcription factors, like Arnt1 and Arnt2, to initiate
307 gene transcription . To determine if Npas4l forms a complex with either Arnt1 or Arnt2, we performed a
308 coimmunoprecipitation experiment. Due to the absence of commercially available antibodies that
309 recognize zebrafish Npas4l, Arnt1 or Arnt2 proteins, we co-expressed tagged versions of zebrafish
310 *npas4l* (Npas4l-V5), *arnt1* (Arnt1-myc), and *arnt2* (Arnt2-HA) in HEK293T cells. We performed co-
311 immunoprecipitation studies and found that Arnt1-myc interacts with Npas4l-V5 and that Arnt2-HA
312 interacts with Npas4l-V5 (**Fig. 4A, B**). These data suggest that Npas4l uses either Arnt1 or Arnt2 or
313 both as a binding partner. Furthermore, these data indicate that Arnt1 and Arnt2 may be functionally
314 interchangeable and redundant, at least in the case of Npas4l.
315

316 **Arnt1 and Arnt2 cannot functionally compensate for one another in the case of Ahr2**

317 Our results demonstrate that Arnt1 and Arnt2 are functionally interchangeable and redundant
318 when it comes to interacting with Npas4l in the context of hemato-vascular development. It is unclear if
319 Arnt1 and Arnt2 are functionally interchangeable with all Class I bHLH-PAS domain transcription factors
320 or just with Npas4l. To determine if *arnt1/arnt2* redundancy is unique to Npas4l, we examined if *arnt1*
321 and *arnt2* are interchangeable in the case of a different class I bHLH-PAS transcription factor, the aryl
322 hydrocarbon receptor 2 (Ahr2). Previous studies demonstrate that Ahr2 can bind DNA in the presence
323 of either Arnt1 or Arnt2 *in vitro* (Andreasen et al., 2002; Hirose et al., 1996; Tanguay et al., 2000), but
324 whether Arnt1 and Arnt2 bind Ahr2 interchangeably *in vivo* is not known. Ahr2 is a ligand-dependent
325 transcription factor. A known ligand of Ahr2 is 2,3,7,8-tetrachlorodibenzo-p-dioxin (TCDD), which we
326 have previously shown induces cardiotoxicity in zebrafish larvae and requires wild-type *ahr2* (Souder
327 and Gorelick, 2019*)*. We asked whether TCDD causes cardiotoxicity in *arnt1* or *arnt2* single mutants,
328 reasoning that if Ahr2 interacts with Arnt1 or Arnt2 interchangeably, then only *arnt1/2* double mutants,
329 but not single mutants, would be resistant to TCDD exposure. We treated wildtype, *arnt1* mutants, and
330 *arnt2* mutants with either vehicle (0.1% DMSO) (**Fig. 5A, B, and C**) or with 10 ng/mL TCDD (**Fig. 5D,**
331 **E, and F**) from 1 dpf to 3 dpf. Wildtype and *arnt2* mutants treated with TCDD exhibit cardiac edema and
332 the heart fails to loop properly (**Fig. 5D,** and **F**), unlike vehicle treated siblings (**Fig. 5A** and **C**). In
333 contrast, *arnt1* mutants treated with TCDD showed normal heart looping and lack cardiac edema (**Fig.**
334 **5E**), like their vehicle treated siblings (**Fig. 5B**). This suggests that *arnt1,* but not *arnt2,* is required for
335 Ahr2-dependent TCDD toxicity. This also shows that *arnt1* and *arnt2* are not always redundant *in vivo*
336 and that the Class I dimerization partner may influence whether the Class II dimerization partners are
337 redundant.
338

339 **DISCUSSION**

340 Class I bHLH-PAS proteins must dimerize with Class II bHLH-PAS proteins to transcribe
341 their target genes (Ema et al., 1996; Erbel et al., 2003; Jiang et al., 1996; Lees and Whitelaw,
342 1999; Michaud et al., 2000; Wu and Rastinejad, 2017). It has previously been established that
343 Npas4l, a Class I bHLH-PAS transcription factor, is required for hemato-vascular development
344 in zebrafish (Reischauer et al., 2016). To determine the Class II bHLH-PAS binding partner of
345 Npas4l, we generated *arnt1* mutant and *arnt2* mutant zebrafish and expected one of these
346 mutants to mimic the *npas4l* mutant phenotype. However, both *arnt1* mutant and *arnt2* mutant
347 larvae are viable to 5dpf and are indistinguishable from wildtype embryos by eye. Our results
348 demonstrate that double homozygous *arnt1/2* mutant embryos have a similar phenotype to
349 *npas4l* mutants (Reischauer et al., 2016; Stainier et al., 1995b; Thompson et al., 1998) and
350 that Npas4l can function with either Arnt1 or Arnt2. Thus, Arnt1 and Arnt2 act redundantly to
351 specify hemato-vascular progenitor cells.

352 Endothelial cell development and hematopoietic cell development are closely related during
353 embryogenesis. Both cell types primarily arise from the lateral plate mesoderm (LPM) and
354 share a common progenitor (Qian et al., 2005; Reischauer et al., 2016; Stainier et al., 1995a;
355 Thompson et al., 1998). Additionally, during definitive hematopoiesis, some HSCs are derived
356 from specialized endothelial cells, called hemogenic endothelium (Boisset et al., 2010; Kissa
357 and Herbomel, 2010). Both *npas4l* and *arnt1/2* mutants lack all blood cells but do have a small
358 population of endothelial cells, which is restricted to the most posterior region of the animal
359 (Figure 2 and (Reischauer et al., 2016)). In zebrafish, there is a population of endothelial cells
360 in the caudal region of the embryo that are not derived from the LPM and differentiate in the
361 absence of *npas4l* expression (Pak et al., 2020). We hypothesize that *arnt1* and *arnt2* are

362 required for the differentiation of endothelial cells from the LPM but are not required for the
363 differentiation of endothelial cells, such as the caudal population, from outside the LPM. The
364 transcriptomic signature of the caudal population of endothelial cells was distinct from
365 endothelial cells that require *npas4l* for differentiation, with genes for somitogenesis and
366 neurogenesis highly enriched compared to LPM-derived endothelial cells (Pak et al., 2020).
367 Based on this transcriptome analysis, we speculate that the caudal population of endothelial
368 cells fails to express genes required for hemogenic endothelium and that no blood cells are
369 derived from the caudal population of endothelial cells. This is consistent with the observation
370 that the caudal population of endothelial cells, but not blood cells, are present in *npas4l* or
371 *arnt1/2* mutants.

372 Our results show that either Arnt1 or Arnt2, Class II bHLH-PAS proteins, can act as a
373 required co-factor for Npas4l-dependent mesodermal specification to hematopoietic and
374 endothelial progenitors. Likewise, Arnt1 is essential for adult hematopoietic stem cells in mice
375 and is required for survival of hematopoietic progenitor cells in the fetal liver (Krock et al.,
376 2015). Homozygous Arnt1 mutant mice are not viable beyond E10.5 and show severe defects
377 in vascularization, suggesting that Arnt1 is essential for normal vascular development (Kozak
378 et al., 1997; Maltepe et al., 1997). The role of Arnt1 during mammalian embryonic
379 hematopoiesis remains unclear.

380 Based on these data we speculate that the mammalian equivalent to zebrafish Npas4l
381 is likely to be a Class I bHLH-PAS protein that heterodimerizes with ARNT1. Zebrafish Npas4l
382 shows the most sequence homology to mouse Npas4 (Reischauer et al., 2016). Although
383 Npas4 is known to dimerize with Arnt1 and Arnt2 *in vivo* (Brigidi et al., 2019), mammalian
384 Npas4 is unlikely to be the functional equivalent to zebrafish Npas4l because homozygous

385 Npas4 mutant mice are viable to adulthood and do not show any overt vascular or
386 hematopoietic defects (Bloodgood et al., 2013).
387 Similarly, we speculate that Npas1, 2, and 3 are unlikely to be the mammalian
388 equivalent to Npas4l, as mice mutant for these genes are viable to adulthood and no
389 endothelial or hematopoietic phenotype has been reported (Dudley et al., 2003; Erbel-Sieler et
390 al., 2004). Additionally, we think that the Sim (Sim1/2) and Circadian Locomotor Output Cycles
391 Kaput (CLOCK) genes are unlikely to the be the master regulators of hemato-vascular
392 specification in mice or humans because mutant mice appear to have normal blood cells and
393 vasculature (DeBruyne et al., 2007; Epstein et al., 2000; Holder et al., 2004). We cannot
394 exclude the possibility that Npas1, 2, 3 and 4 proteins act redundantly to specify hemato-
395 vascular progenitors in mammalian embryos because mice with mutations in multiple Npas
396 genes have not been reported.
397 Three other Class I bHLH-PAS proteins, Ahr, Hif1α, and Hif2α, are known to be
398 involved in mammalian hematopoiesis and vascularization. Lack of Ahr *in vitro* and *in vivo*
399 promotes adult hematopoietic progenitor expansion and resulted in aberrant ratios and
400 functionality of some blood cell populations, suggesting that Ahr could be functionally relevant
401 during definitive hematopoiesis (Singh et al., 2011; Smith et al., 2013). However, there is no
402 evidence that Ahr is expressed during primitive hematopoiesis in mice and Ahr mutant mice
403 are viable to adulthood and do not show any vascular defects (Singh et al., 2011).
404 Hif1α and Hif2α are involved in mouse vascular development and hematopoiesis (Iyer
405 et al., 1998; Krock et al., 2015; Peng et al., 2000; Scortegagna et al., 2003; Takubo et al.,
406 2010). However, the role of Hif1α and Hif2α during early mouse embryonic hematopoiesis and
407 endothelial development is not well characterized. Hif1α is required for cell cycle quiescence of

408 adult hematopoietic stem cells (Takubo et al., 2010). Hif1α mRNA is detected during mouse
409 primitive hematopoiesis and Hif1α homozygous mutant mice die *in utero* before E11.5 (Iyer et
410 al., 1998; Kotch et al., 1999). The Hif1α mutant mice are reported to have defects in blood
411 vessels, increased death of vascular-supporting mesenchymal cells, and cardiovascular
412 defects (Iyer et al., 1998; Kotch et al., 1999). In mice, Hif2α mRNA is expressed during primary
413 hematopoiesis specifically within the yolk sac, where primary hematopoiesis originates
414 (Flamme et al., 1997). Global knockout of *Hif2α* is reported to be embryonic or postnatal lethal
415 depending upon the mutation and strain of mouse used (Compernolle et al., 2002; Peng et al.,
416 2000; Tian et al., 1998). Embryonic lethal Hif2α mutants showed severe vascular
417 disorganization and increased frequency of hemorrhaging *in utero* (Compernolle et al., 2002;
418 Peng et al., 2000). Both *Hif1α* and *Hif2α* mutants have endothelial and blood cells, thus neither
419 mutation mimics the zebrafish *npas4l* phenotype. But both *Hif1α* and *Hif2α* mutant mice do
420 have a vascular phenotype (Compernolle et al., 2002; Compernolle et al., 2003; Iyer et al.,
421 1998; Peng et al., 2000; Ryan et al., 1998). Although neither Hif1α nor Hif2α single mutant
422 mice recapitulate the phenotype observed in zebrafish *cloche* or *arnt1;arnt2* mutants, the HIFs
423 are strong candidates to be the functional equivalent of Npas4l.
424 One reason we may not see an Npas4l-like phenotype in Hif1α or Hif2α single mutant
425 mice could be because of genetic compensation. Genetic compensation occurs in both
426 zebrafish and mice (Bunton-Stasyshyn et al., 2019; Rossi et al., 2015). There is evidence in
427 zebrafish and mice of *Hif1α* and *Hif2α* functionally compensating for one another. Zebrafish
428 with reduced expression of all 4 Hif1 and Hif2 transcripts *(hif1aa, hif1ab, hif2aa, hif2ab*) lack
429 hemogenic endothelium, suggesting that at least one HIF gene is required for the specification
430 of hemogenic endothelium (Gerri et al., 2018). These results also indicate that *hif1α* and *hif2α*

431 are functionally redundant for the generation of hemogenic endothelium (Gerri et al., 2018).
432 Global knockout of mouse *Hif1α* is embryonic lethal (Compernolle et al., 2003; Iyer et al., 1998;
433 Ryan et al., 1998) and global knockout of mouse *Hif2α* is embryonic or postnatal lethal
434 depending upon the strain of mouse used (Compernolle et al., 2002; Peng et al., 2000; Tian et
435 al., 1998).

436 To our knowledge, no one has generated a mouse in which both *Hif1α* and *Hif2α* are
437 globally knocked-out. Future studies could examine if global or mesodermal-specific knockout
438 of both *Hif1α* and *Hif2α* genes in mouse results in a phenotype similar to knockout of both
439 *arnt1* and *arnt2* in zebrafish. Our results demonstrate that under some conditions, Arnt1 and
440 Arnt2 act redundantly. In other contexts, Arnt1 is the preferred binding protein for a class I PAS
441 transcription factor. The extent to which this occurs during different developmental stages *in*
442 *vivo*, or in different cell types, warrants further study.

443

444 **Acknowledgements**

445 We thank Lauren Pandolfo and the staff of the Baylor College of Medicine aquatics facility for taking
446 care of our zebrafish colony. This work funded by NIH grants R01ES026337 and P30ES030285.

447 References:
448

449 Andreasen, E.A., Hahn, M.E., Heideman, W., Peterson, R.E., Tanguay, R.L., 2002. The zebrafish
450 (Danio rerio) aryl hydrocarbon receptor type 1 is a novel vertebrate receptor. Molecular pharmacology
451 62, 234-249.

452 Aplan, P.D., Nakahara, K., Orkin, S.H., Kirsch, I.R., 1992. The SCL gene product: a positive regulator
453 of erythroid differentiation. The EMBO journal 11, 4073-4081.

454 Bloodgood, B.L., Sharma, N., Browne, H.A., Trepman, A.Z., Greenberg, M.E., 2013. The activity-
455 dependent transcription factor NPAS4 regulates domain-specific inhibition. Nature 503, 121-125.

456 Boisset, J.C., van Cappellen, W., Andrieu-Soler, C., Galjart, N., Dzierzak, E., Robin, C., 2010. In vivo
457 imaging of haematopoietic cells emerging from the mouse aortic endothelium. Nature 464, 116-120.

458 Brigidi, G.S., Hayes, M.G.B., Delos Santos, N.P., Hartzell, A.L., Texari, L., Lin, P.A., Bartlett, A., Ecker,
459 J.R., Benner, C., Heinz, S., Bloodgood, B.L., 2019. Genomic Decoding of Neuronal Depolarization by
460 Stimulus-Specific NPAS4 Heterodimers. Cell 179, 373-391 e327.

461 Brownlie, A., Donovan, A., Pratt, S.J., Paw, B.H., Oates, A.C., Brugnara, C., Witkowska, H.E., Sassa,
462 S., Zon, L.I., 1998. Positional cloning of the zebrafish sauternes gene: a model for congenital
463 sideroblastic anaemia. Nat Genet 20, 244-250.

464 Bunton-Stasyshyn, R.K.A., Wells, S., Teboul, L., 2019. When all is not lost: considering genetic
465 compensation in laboratory animals. Lab Anim (NY) 48, 282-284.

466 Casie Chetty, S., Rost, M.S., Enriquez, J.R., Schumacher, J.A., Baltrunaite, K., Rossi, A., Stainier,
467 D.Y., Sumanas, S., 2017. Vegf signaling promotes vascular endothelial differentiation by modulating
468 etv2 expression. Dev Biol 424, 147-161.

469 Compernolle, V., Brusselmans, K., Acker, T., Hoet, P., Tjwa, M., Beck, H., Plaisance, S., Dor, Y.,
470 Keshet, E., Lupu, F., Nemery, B., Dewerchin, M., Van Veldhoven, P., Plate, K., Moons, L., Collen, D.,
471 Carmeliet, P., 2002. Loss of HIF-2alpha and inhibition of VEGF impair fetal lung maturation, whereas
472 treatment with VEGF prevents fatal respiratory distress in premature mice. Nat Med 8, 702-710.

473 Compernolle, V., Brusselmans, K., Franco, D., Moorman, A., Dewerchin, M., Collen, D., Carmeliet, P.,
474 2003. Cardia bifida, defective heart development and abnormal neural crest migration in embryos
475 lacking hypoxia-inducible factor-1alpha. Cardiovasc Res 60, 569-579.

476 Costa, G., Kouskoff, V., Lacaud, G., 2012. Origin of blood cells and HSC production in the embryo.
477 Trends Immunol 33, 215-223.

478 DeBruyne, J.P., Weaver, D.R., Reppert, S.M., 2007. CLOCK and NPAS2 have overlapping roles in the
479 suprachiasmatic circadian clock. Nat Neurosci 10, 543-545.

480 Dobrzycki, T., Krecsmarik, M., Bonkhofer, F., Patient, R., Monteiro, R., 2018. An optimised pipeline for
481 parallel image-based quantification of gene expression and genotyping after in situ hybridisation. Biol
482 Open 7.

483 Dooley, K.A., Davidson, A.J., Zon, L.I., 2005. Zebrafish scl functions independently in hematopoietic
484 and endothelial development. Dev Biol 277, 522-536.

485 Doss, M.X., Gaspar, J.A., Winkler, J., Hescheler, J., Schulz, H., Sachinidis, A., 2012. Specific gene
486 signatures and pathways in mesodermal cells and their derivatives derived from embryonic stem cells.
487 Stem Cell Rev Rep 8, 43-54.

488 Dudley, C.A., Erbel-Sieler, C., Estill, S.J., Reick, M., Franken, P., Pitts, S., McKnight, S.L., 2003.
489 Altered patterns of sleep and behavioral adaptability in NPAS2-deficient mice. Science 301, 379-383.

490 Dumont, D.J., Fong, G.H., Puri, M.C., Gradwohl, G., Alitalo, K., Breitman, M.L., 1995. Vascularization of
491 the mouse embryo: a study of flk-1, tek, tie, and vascular endothelial growth factor expression during
492 development. Dev Dyn 203, 80-92.

493 Ema, M., Morita, M., Ikawa, S., Tanaka, M., Matsuda, Y., Gotoh, O., Saijoh, Y., Fujii, H., Hamada, H.,
494 Kikuchi, Y., Fujii-Kuriyama, Y., 1996. Two new members of the murine Sim gene family are
495 transcriptional repressors and show different expression patterns during mouse embryogenesis.
496 Molecular and cellular biology 16, 5865-5875.

497 Epstein, D.J., Martinu, L., Michaud, J.L., Losos, K.M., Fan, C., Joyner, A.L., 2000. Members of the
498 bHLH-PAS family regulate Shh transcription in forebrain regions of the mouse CNS. Development 127,
499 4701-4709.

500 Erbel, P.J., Card, P.B., Karakuzu, O., Bruick, R.K., Gardner, K.H., 2003. Structural basis for PAS
501 domain heterodimerization in the basic helix--loop--helix-PAS transcription factor hypoxia-inducible
502 factor. Proc Natl Acad Sci U S A 100, 15504-15509.

503 Erbel-Sieler, C., Dudley, C., Zhou, Y., Wu, X., Estill, S.J., Han, T., Diaz-Arrastia, R., Brunskill, E.W.,
504 Potter, S.S., McKnight, S.L., 2004. Behavioral and regulatory abnormalities in mice deficient in the
505 NPAS1 and NPAS3 transcription factors. Proc Natl Acad Sci U S A 101, 13648-13653.

506 Ferrara, N., Carver-Moore, K., Chen, H., Dowd, M., Lu, L., O'Shea, K.S., Powell-Braxton, L., Hillan,
507 K.J., Moore, M.W., 1996. Heterozygous embryonic lethality induced by targeted inactivation of the
508 VEGF gene. Nature 380, 439-442.

509 Flamme, I., Frohlich, T., von Reutern, M., Kappel, A., Damert, A., Risau, W., 1997. HRF, a putative
510 basic helix-loop-helix-PAS-domain transcription factor is closely related to hypoxia-inducible factor-1
511 alpha and developmentally expressed in blood vessels. Mech Dev 63, 51-60.

512 Gerri, C., Marass, M., Rossi, A., Stainier, D.Y.R., 2018. Hif-1alpha and Hif-2alpha regulate hemogenic
513 endothelium and hematopoietic stem cell formation in zebrafish. Blood 131, 963-973.

514 Gong, B., Liang, D., Chew, T.G., Ge, R., 2004. Characterization of the zebrafish vascular endothelial
515 growth factor A gene: comparison with vegf-A genes in mammals and Fugu. Biochim Biophys Acta
516 1676, 33-40.

517 Gunaseeli, I., Doss, M.X., Antzelevitch, C., Hescheler, J., Sachinidis, A., 2010. Induced pluripotent
518 stem cells as a model for accelerated patient- and disease-specific drug discovery. Curr Med Chem 17,
519 759-766.

520 Hill, A.J., Heiden, T.C., Heideman, W., Peterson, R.E., 2009. Potential roles of Arnt2 in zebrafish larval
521 development. Zebrafish 6, 79-91.

522 Hirose, K., Morita, M., Ema, M., Mimura, J., Hamada, H., Fujii, H., Saijo, Y., Gotoh, O., Sogawa, K.,
523 Fujii-Kuriyama, Y., 1996. cDNA cloning and tissue-specific expression of a novel basic helix-loop-
524 helix/PAS factor (Arnt2) with close sequence similarity to the aryl hydrocarbon receptor nuclear
525 translocator (Arnt). Molecular and cellular biology 16, 1706-1713.

526 Hirschi, K.K., 2012. Hemogenic endothelium during development and beyond. Blood 119, 4823-4827.

527 Holder, J.L., Jr., Zhang, L., Kublaoui, B.M., DiLeone, R.J., Oz, O.K., Bair, C.H., Lee, Y.H., Zinn, A.R.,
528 2004. Sim1 gene dosage modulates the homeostatic feeding response to increased dietary fat in mice.
529 American journal of physiology. Endocrinology and metabolism 287, E105-113.

530 Huber, T.L., Kouskoff, V., Fehling, H.J., Palis, J., Keller, G., 2004. Haemangioblast commitment is
531 initiated in the primitive streak of the mouse embryo. Nature 432, 625-630.

532 Hughes, M.C., Zimmer, A.M., Perry, S.F., 2019. Role of internal convection in respiratory gas transfer
533 and aerobic metabolism in larval zebrafish (Danio rerio). Am J Physiol Regul Integr Comp Physiol 316,
534 R255-R264.

535 Iyer, N.V., Kotch, L.E., Agani, F., Leung, S.W., Laughner, E., Wenger, R.H., Gassmann, M., Gearhart,
536 J.D., Lawler, A.M., Yu, A.Y., Semenza, G.L., 1998. Cellular and developmental control of O2
537 homeostasis by hypoxia-inducible factor 1 alpha. Genes & development 12, 149-162.

538 Jao, L.E., Wente, S.R., Chen, W., 2013. Efficient multiplex biallelic zebrafish genome editing using a
539 CRISPR nuclease system. Proc Natl Acad Sci U S A 110, 13904-13909.

540 Jiang, B.H., Rue, E., Wang, G.L., Roe, R., Semenza, G.L., 1996. Dimerization, DNA binding, and
541 transactivation properties of hypoxia-inducible factor 1. J Biol Chem 271, 17771-17778.

542 Kalev-Zylinska, M.L., Horsfield, J.A., Flores, M.V., Postlethwait, J.H., Vitas, M.R., Baas, A.M., Crosier,
543 P.S., Crosier, K.E., 2002a. Runx1 is required for zebrafish blood and vessel development and
544 expression of a human RUNX1-CBF2T1 transgene advances a model for studies of leukemogenesis.
545 Development 129, 2015-2030.

546 Kalev-Zylinska, M.L., Horsfield, J.A., Flores, M.V.C., Postlethwait, J.H., Vitas, M.R., Baas, A.M.,
547 Crosier, P.S., Crosier, K.E., 2002b. Runx1 is required for zebrafish blood and vessel development and
548 expression of a human RUNX1-CBF2T1 transgene advances a model for studies of leukemogenesis.
549 Development 129, 2015-2030.

550 Kataoka, H., Hayashi, M., Nakagawa, R., Tanaka, Y., Izumi, N., Nishikawa, S., Jakt, M.L., Tarui, H.,
551 Nishikawa, S., 2011. Etv2/ER71 induces vascular mesoderm from Flk1+PDGFRalpha+ primitive
552 mesoderm. Blood 118, 6975-6986.

553 Kissa, K., Herbomel, P., 2010. Blood stem cells emerge from aortic endothelium by a novel type of cell
554 transition. Nature 464, 112-115.

555 Kobayashi, I., Kobayashi-Sun, J., Kim, A.D., Pouget, C., Fujita, N., Suda, T., Traver, D., 2014. Jam1a-
556 Jam2a interactions regulate haematopoietic stem cell fate through Notch signalling. Nature 512, 319-
557 323.

558 Kotch, L.E., Iyer, N.V., Laughner, E., Semenza, G.L., 1999. Defective vascularization of HIF-1alpha-null
559 embryos is not associated with VEGF deficiency but with mesenchymal cell death. Dev Biol 209, 254-
560 267.

561 Kozak, K.R., Abbott, B., Hankinson, O., 1997. ARNT-deficient mice and placental differentiation. Dev
562 Biol 191, 297-305.

563 Krock, B.L., Eisinger-Mathason, T.S., Giannoukos, D.N., Shay, J.E., Gohil, M., Lee, D.S., Nakazawa,
564 M.S., Sesen, J., Skuli, N., Simon, M.C., 2015. The aryl hydrocarbon receptor nuclear translocator is an
565 essential regulator of murine hematopoietic stem cell viability. Blood 125, 3263-3272.

566 Labun, K., Montague, T.G., Gagnon, J.A., Thyme, S.B., Valen, E., 2016. CHOPCHOP v2: a web tool
567 for the next generation of CRISPR genome engineering. Nucleic Acids Res 44, W272-276.

568 Labun, K., Montague, T.G., Krause, M., Torres Cleuren, Y.N., Tjeldnes, H., Valen, E., 2019.
569 CHOPCHOP v3: expanding the CRISPR web toolbox beyond genome editing. Nucleic Acids Res 47,
570 W171-W174.

571 Lam, E.Y., Chau, J.Y., Kalev-Zylinska, M.L., Fountaine, T.M., Mead, R.S., Hall, C.J., Crosier, P.S.,
572 Crosier, K.E., Flores, M.V., 2009. Zebrafish runx1 promoter-EGFP transgenics mark discrete sites of
573 definitive blood progenitors. Blood 113, 1241-1249.

574 Lauter, G., Soll, I., Hauptmann, G., 2011. Multicolor fluorescent in situ hybridization to define abutting
575 and overlapping gene expression in the embryonic zebrafish brain. Neural Dev 6, 10.

576 Lee, R.K., Stainier, D.Y., Weinstein, B.M., Fishman, M.C., 1994. Cardiovascular development in the
577 zebrafish. II. Endocardial progenitors are sequestered within the heart field. Development 120, 3361-
578 3366.

579 Lees, M.J., Whitelaw, M.L., 1999. Multiple roles of ligand in transforming the dioxin receptor to an active
580 basic helix-loop-helix/PAS transcription factor complex with the nuclear protein Arnt. Molecular and
581 cellular biology 19, 5811-5822.

582 Liao, E.C., Paw, B.H., Oates, A.C., Pratt, S.J., Postlethwait, J.H., Zon, L.I., 1998. SCL/Tal-1
583 transcription factor acts downstream of cloche to specify hematopoietic and vascular progenitors in
584 zebrafish. Genes & development 12, 621-626.

585 Liao, W., Bisgrove, B.W., Sawyer, H., Hug, B., Bell, B., Peters, K., Grunwald, D.J., Stainier, D.Y., 1997.
586 The zebrafish gene cloche acts upstream of a flk-1 homologue to regulate endothelial cell
587 differentiation. Development 124, 381-389.

588 Liao, W., Ho, C.Y., Yan, Y.L., Postlethwait, J., Stainier, D.Y., 2000. Hhex and scl function in parallel to
589 regulate early endothelial and blood differentiation in zebrafish. Development 127, 4303-4313.

590 Lohr, H., Ryu, S., Driever, W., 2009. Zebrafish diencephalic A11-related dopaminergic neurons share a
591 conserved transcriptional network with neuroendocrine cell lineages. Development 136, 1007-1017.

592 Maltepe, E., Schmidt, J.V., Baunoch, D., Bradfield, C.A., Simon, M.C., 1997. Abnormal angiogenesis
593 and responses to glucose and oxygen deprivation in mice lacking the protein ARNT. Nature 386, 403-
594 407.

595 Marchi, D., Santhakumar, K., Markham, E., Li, N., Storbeck, K.H., Krone, N., Cunliffe, V.T., van Eeden,
596 F.J.M., 2020. Bidirectional crosstalk between Hypoxia-Inducible Factor and glucocorticoid signalling in
597 zebrafish larvae. PLoS Genet 16, e1008757.

598 Michaud, J.L., DeRossi, C., May, N.R., Holdener, B.C., Fan, C.M., 2000. ARNT2 acts as the
599 dimerization partner of SIM1 for the development of the hypothalamus. Mech Dev 90, 253-261.

600 Moore, C., Richens, J.L., Hough, Y., Ucanok, D., Malla, S., Sang, F., Chen, Y., Elworthy, S., Wilkinson,
601 R.N., Gering, M., 2018. Gfi1aa and Gfi1b set the pace for primitive erythroblast differentiation from
602 hemangioblasts in the zebrafish embryo. Blood Adv 2, 2589-2606.

603 Moore, J.C., Sheppard-Tindell, S., Shestopalov, I.A., Yamazoe, S., Chen, J.K., Lawson, N.D., 2013.
604 Post-transcriptional mechanisms contribute to Etv2 repression during vascular development. Dev Biol
605 384, 128-140.

606 Okuda, T., van Deursen, J., Hiebert, S.W., Grosveld, G., Downing, J.R., 1996. AML1, the target of
607 multiple chromosomal translocations in human leukemia, is essential for normal fetal liver
608 hematopoiesis. Cell 84, 321-330.

609 Paik, E.J., Zon, L.I., 2010. Hematopoietic development in the zebrafish. Int J Dev Biol 54, 1127-1137.

610 Pak, B., Schmitt, C.E., Choi, W., Kim, J.D., Han, O., Alsio, J., Jung, D.W., Williams, D.R., Coppieters,
611 W., Stainier, D.Y.R., Jin, S.W., 2020. Analyses of Avascular Mutants Reveal Unique Transcriptomic
612 Signature of Non-conventional Endothelial Cells. Front Cell Dev Biol 8, 589717.

613 Palis, J., Robertson, S., Kennedy, M., Wall, C., Keller, G., 1999. Development of erythroid and myeloid
614 progenitors in the yolk sac and embryo proper of the mouse. Development 126, 5073-5084.

615 Parant, J.M., George, S.A., Pryor, R., Wittwer, C.T., Yost, H.J., 2009. A rapid and efficient method of
616 genotyping zebrafish mutants. Dev Dyn 238, 3168-3174.

617 Pelster, B., Burggren, W.W., 1996. Disruption of hemoglobin oxygen transport does not impact oxygen-
618 dependent physiological processes in developing embryos of zebra fish (Danio rerio). Circulation
619 Research 79, 358-362.

620 Peng, J., Zhang, L., Drysdale, L., Fong, G.H., 2000. The transcription factor EPAS-1/hypoxia-inducible
621 factor 2alpha plays an important role in vascular remodeling. Proc Natl Acad Sci U S A 97, 8386-8391.

622 Pongratz, I., Antonsson, C., Whitelaw, M.L., Poellinger, L., 1998. Role of the PAS domain in regulation
623 of dimerization and DNA binding specificity of the dioxin receptor. Mol Cell Biol 18.

624 Prasch, A.L., Tanguay, R.L., Mehta, V., Heideman, W., Peterson, R.E., 2006. Identification of zebrafish
625 ARNT1 homologs: 2,3,7,8-tetrachlorodibenzo-p-dioxin toxicity in the developing zebrafish requires
626 ARNT1. Molecular pharmacology 69, 776-787.

627 Qian, F., Zhen, F., Ong, C., Jin, S.W., Meng Soo, H., Stainier, D.Y., Lin, S., Peng, J., Wen, Z., 2005.
628 Microarray analysis of zebrafish cloche mutant using amplified cDNA and identification of potential
629 downstream target genes. Dev Dyn 233, 1163-1172.

630 Reischauer, S., Stone, O.A., Villasenor, A., Chi, N., Jin, S.W., Martin, M., Lee, M.T., Fukuda, N.,
631 Marass, M., Witty, A., Fiddes, I., Kuo, T., Chung, W.S., Salek, S., Lerrigo, R., Alsio, J., Luo, S., Tworus,

632 D., Augustine, S.M., Mucenieks, S., Nystedt, B., Giraldez, A.J., Schroth, G.P., Andersson, O., Stainier,
633 D.Y., 2016. Cloche is a bHLH-PAS transcription factor that drives haemato-vascular specification.
634 Nature 535, 294-298.

635 Romano, S.N., Edwards, H.E., Souder, J.P., Ryan, K.J., Cui, X., Gorelick, D.A., 2017. G protein-
636 coupled estrogen receptor regulates embryonic heart rate in zebrafish. PLoS Genet 13, e1007069.

637 Rossi, A., Kontarakis, Z., Gerri, C., Nolte, H., Holper, S., Kruger, M., Stainier, D.Y., 2015. Genetic
638 compensation induced by deleterious mutations but not gene knockdowns. Nature 524, 230-233.

639 Ryan, H.E., Lo, J., Johnson, R.S., 1998. HIF-1 alpha is required for solid tumor formation and
640 embryonic vascularization. The EMBO journal 17, 3005-3015.

641 Scortegagna, M., Morris, M.A., Oktay, Y., Bennett, M., Garcia, J.A., 2003. The HIF family member
642 EPAS1/HIF-2alpha is required for normal hematopoiesis in mice. Blood 102, 1634-1640.

643 Shalaby, F., Rossant, J., Yamaguchi, T.P., Gertsenstein, M., Wu, X.F., Breitman, M.L., Schuh, A.C.,
644 1995. Failure of blood-island formation and vasculogenesis in Flk-1-deficient mice. Nature 376, 62-66.

645 Shu, L.P., Zhou, Z.W., Zhou, T., Deng, M., Dong, M., Chen, Y., Fu, Y.F., Jin, Y., Zhou, S.F., He, Z.X.,
646 2015. Ectopic expression of Hoxb4a in hemangioblasts promotes hematopoietic development in early
647 embryogenesis of zebrafish. Clinical and experimental pharmacology & physiology 42, 1275-1286.

648 Singh, K.P., Garrett, R.W., Casado, F.L., Gasiewicz, T.A., 2011. Aryl Hydrocarbon Receptor-Null Allele
649 Mice Have Hematopoietic Stem/Progenitor Cells with Abnormal Characteristics and Functions. Stem
650 Cells and Development 20, 769-784.

651 Smith, B.W., Rozelle, S.S., Leung, A., Ubellacker, J., Parks, A., Nah, S.K., French, D., Gadue, P.,
652 Monti, S., Chui, D.H., Steinberg, M.H., Frelinger, A.L., Michelson, A.D., Theberge, R., McComb, M.E.,
653 Costello, C.E., Kotton, D.N., Mostoslavsky, G., Sherr, D.H., Murphy, G.J., 2013. The aryl hydrocarbon
654 receptor directs hematopoietic progenitor cell expansion and differentiation. Blood 122, 376-385.

655 Souder, J.P., Gorelick, D.A., 2019. ahr2, But Not ahr1a or ahr1b, Is Required for Craniofacial and Fin
656 Development and TCDD-dependent Cardiotoxicity in Zebrafish. Toxicol Sci 170, 25-44.

657 Stainier, D.Y., Lee, R.K., Fishman, M.C., 1993. Cardiovascular development in the zebrafish. I.
658 Myocardial fate map and heart tube formation. Development 119, 31-40.

659 Stainier, D.Y., Weinstein, B.M., Detrich, H.W., 3rd, Zon, L.I., Fishman, M.C., 1995a. Cloche, an early
660 acting zebrafish gene, is required by both the endothelial and hematopoietic lineages. Development
661 121, 3141-3150.

662 Stainier, D.Y., Weinstein, B.M., Detrich, H.W., Zon, L.I., Fishman, M.C., 1995b. Cloche, an early acting
663 zebrafish gene, is required by both the endothelial and hematopoietic lineages. Development 121,
664 3141-3150.

665 Takubo, K., Goda, N., Yamada, W., Iriuchishima, H., Ikeda, E., Kubota, Y., Shima, H., Johnson, R.S.,
666 Hirao, A., Suematsu, M., Suda, T., 2010. Regulation of the HIF-1alpha level is essential for
667 hematopoietic stem cells. Cell stem cell 7, 391-402.

668 Tanguay, R.L., Andreasen, E., Heideman, W., Peterson, R.E., 2000. Identification and expression of
669 alternatively spliced aryl hydrocarbon nuclear translocator 2 (ARNT2) cDNAs from zebrafish with
670 distinct functions. Biochim Biophys Acta 1494, 117-128.

671 Thisse, C., Thisse, B., 2008. High-resolution in situ hybridization to whole-mount zebrafish embryos.
672 Nat Protoc 3, 59-69.

673 Thompson, M.A., Ransom, D.G., Pratt, S.J., MacLennan, H., Kieran, M.W., Detrich, H.W., 3rd, Vail, B.,
674 Huber, T.L., Paw, B., Brownlie, A.J., Oates, A.C., Fritz, A., Gates, M.A., Amores, A., Bahary, N., Talbot,
675 W.S., Her, H., Beier, D.R., Postlethwait, J.H., Zon, L.I., 1998. The cloche and spadetail genes
676 differentially affect hematopoiesis and vasculogenesis. Dev Biol 197, 248-269.

677 Tian, H., Hammer, R.E., Matsumoto, A.M., Russell, D.W., McKnight, S.L., 1998. The hypoxia-
678 responsive transcription factor EPAS1 is essential for catecholamine homeostasis and protection
679 against heart failure during embryonic development. Genes & development 12, 3320-3324.

680 Vogeli, K.M., Jin, S.W., Martin, G.R., Stainier, D.Y., 2006. A common progenitor for haematopoietic and
681 endothelial lineages in the zebrafish gastrula. Nature 443, 337-339.

682 Wang, Q., Stacy, T., Binder, M., Marin-Padilla, M., Sharpe, A.H., Speck, N.A., 1996. Disruption of the
683 Cbfa2 gene causes necrosis and hemorrhaging in the central nervous system and blocks definitive
684 hematopoiesis. Proceedings of the National Academy of Sciences of the United States of America 93,
685 3444-3449.

686 Weng, W., Nagai, H., Hamidi, S., Sheng, G., 2020. NPAS4L is involved in avian hemangioblast
687 specification. Haematologica.

688 Westerfield, M., 2000. The Zebrafish Book. A Guide for the Laboratory Use of Zebrafish (Danio Rerio).
689 4th ed. University of Oregon Press, Eugene, OR.

690 Wu, D., Rastinejad, F., 2017. Structural characterization of mammalian bHLH-PAS transcription factors.
691 Curr Opin Struct Biol 43, 1-9.

692 Zhang, C., Featherstone, M., 2020. A zebrafish hox gene acts before gastrulation to specify the
693 hemangioblast. Genesis, e23363.
694

695

696

Gene	Allele	CRISPR target	Oligo 1	Oligo 2
arnt1	*bcm1*	GGATGGTTTATAGGTGCCATCGG	TAGGATGGTTTATAGGTGCCAT	AAACATGGCACCTATAAACCAT
arnt1	*bcm2*	GGCGACTGTGAGGATGAGTATGG	TAGGCGACTGTGAGGATGAGTA	AAACTACTCATCCTCACAGTCG
arnt2	*bcm3*	GGTCTCGGTCCGTCTAAGGAGGG	TAGGTCTCGGTCCGTCTAAGGA	AAACTCCTTAGACGGACCGAGA

697

698 Table 1. CRISPR target sequence and oligos used to generate *arnt1* and *arnt2* mutants. PAM sequence in

699 CRISPR target is underlined

700

701

Figure 1

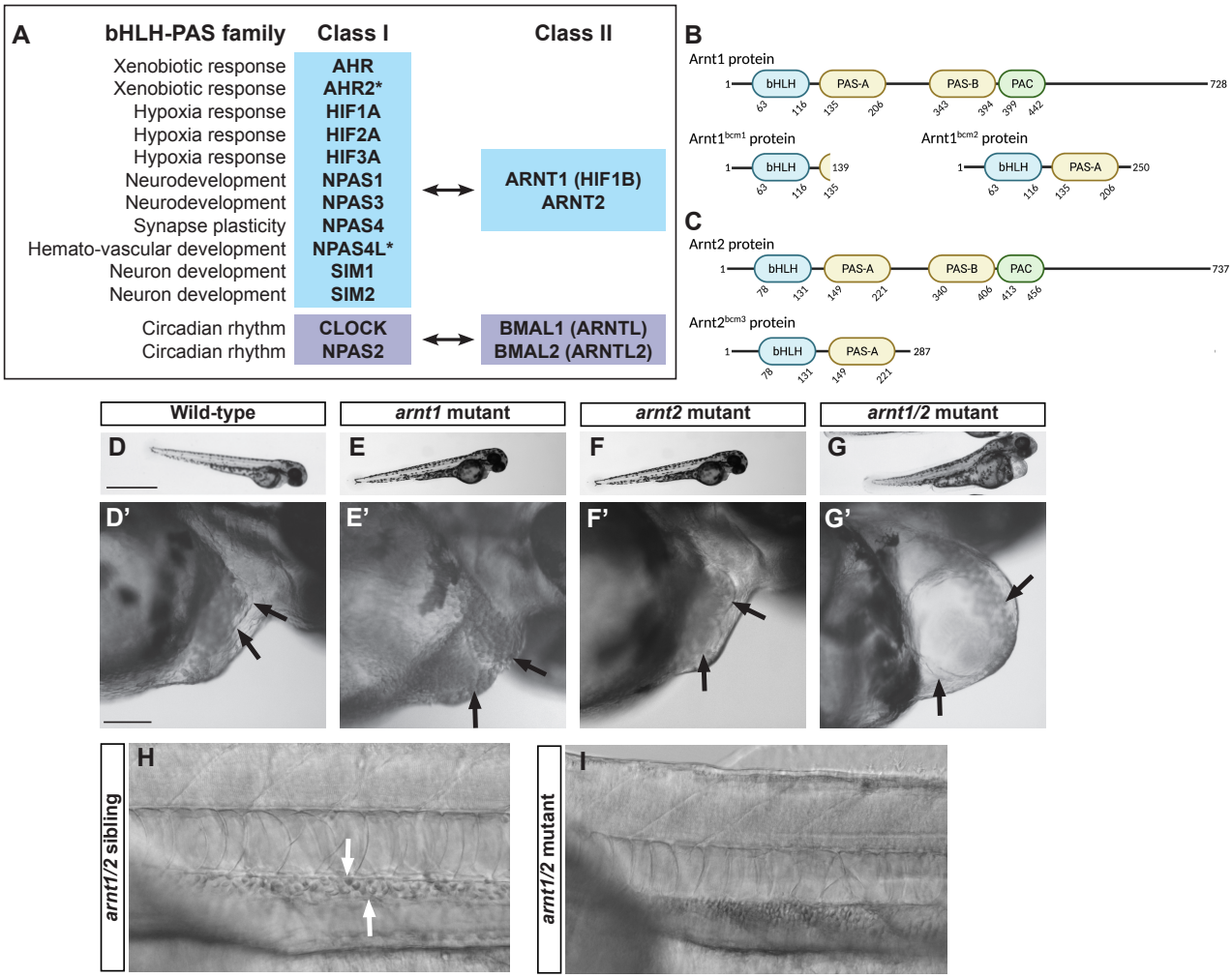

Figure 1. *arnt1*/2 double mutant embryos, but not *arnt1* or *arnt2 single* mutants, lack circulating blood, have cardiac edema and atrial enlargement. (A) bHLH-PAS transcription factors act as heterodimers, where a class I and indicated class II protein interact and bind DNA. Asterisks indicate proteins encoded by genes present in zebrafish but absent in humans. (**B,C**) Generation of zebrafish with mutations in arnt1 and arnt2 genes. The amino acid sequences for the zebrafish Arnt1 (**B**), and Arnt2 proteins (**C**) are represented by the black line. Basic helix-loop-helix (bHLH), Per-Arnt-Sim (PAS) domains, and the motif C-terminally located to the PAS (PAC) are represented by the labeled bubbles. The numbers below each domain indicate the starting and ending amino acid (AA) for each motif. The *arnt1*^{bcm1} mutation causes a premature stop codon to occur at AA139 and loss of the PAS-B, PAC, and majority of the PAS-A. The *arnt1*^{bcm2} mutation causes a premature stop codon to occur at AA250 and loss of the PAS-B and PAC domains (**B**). The *arnt2*^{bcm3} mutation causes a premature stop codon to occur at AA287 and loss of the PAS-B and PAC domains (**C**). (**D-I**) Live embryos from *arnt1*$^{bcm2/+}$;*arnt2*$^{bcm3/+}$ heterozygous parents were imaged at 2 days post fertilization (dpf) prior to genotyping. All double homozygous *arnt1*$^{bcm2/bcm2}$; *arnt2*$^{bcm3/bcm3}$ (*arnt1/2* mutant) embryos showed cardiac edema and atrial enlargement (**G** and **G'**). The wildtype (**D** and **D'**), *arnt1*$^{bcm2/bcm2}$ (*arnt1* mutant) (**E** and **E'**), and *arnt2*$^{bcm3/bcm3}$ (*arnt2* mutant) (**F** and **F'**) siblings of the *arnt1/2* mutants showed normal heart development. Black arrows in panels D'-G' indicate the atrium and ventricle of the heart. Additionally, all siblings of *arnt1/2* mutants had circulating blood (**H** and **M1**) while *arnt1/2* mutants lacked visible circulting blood cells (**I** and **M2**). The white arrows in panel **H** indicate blood cells in the dorsal aorta. Images are representative of 7 different cluches, each cluch contained between 20-300 embryos. For all images of zebrafish embryos (D-I) anterior is towards the right and doral is towards the top of the image. The scale bar in Panel D applies to Panels D-G and is 1000 µm in lenght. The scale bar in Panel D' apples to Panels D'-G' and is 100 µm in length.

705 Figure 2

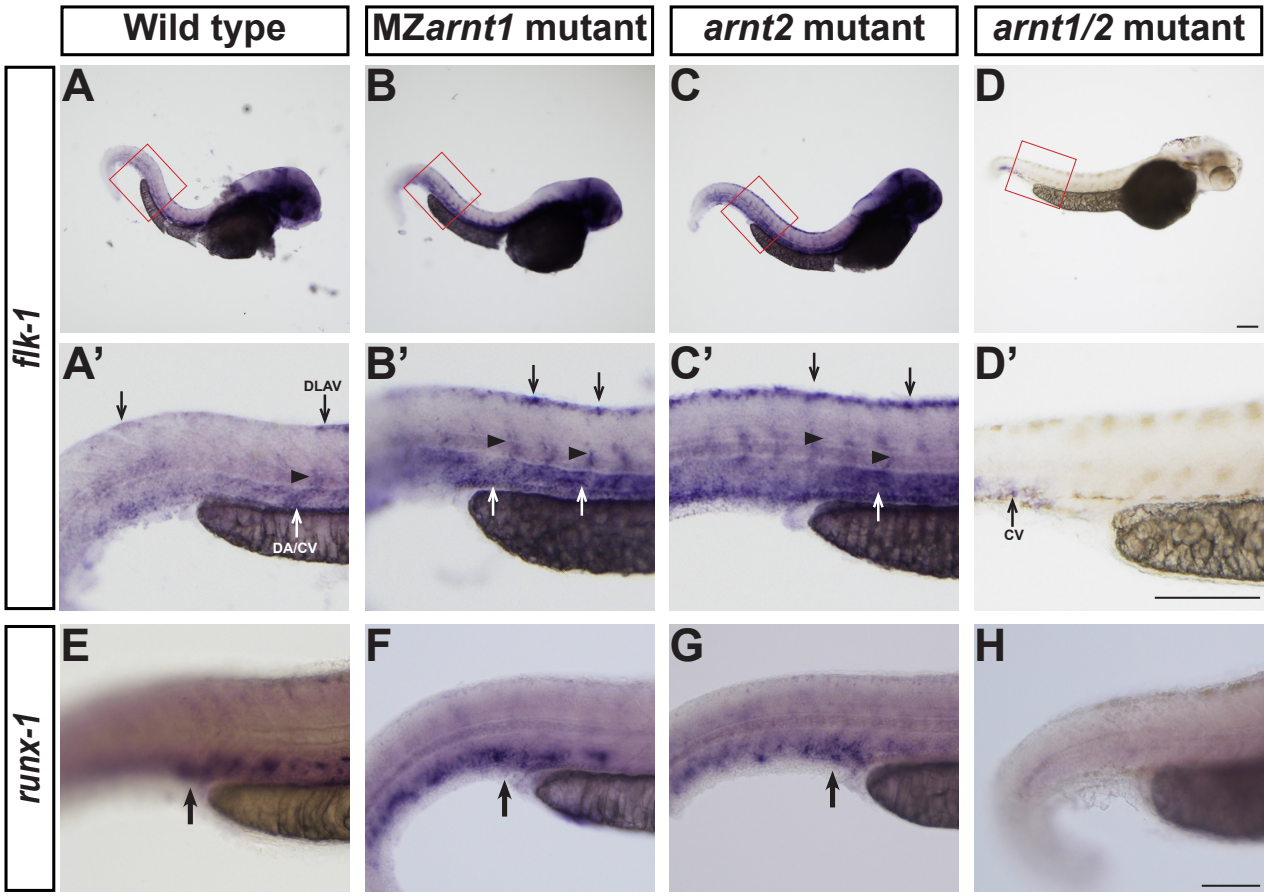

Figure 2. *arnt1/2* double homozygous mutants show reduced levels of *flk-1*-positive endothelial cells and *runx-1*-positive cells in blood island (A-H). Embryos were probed for *flk-1* (A-D) or *runx-1* (E-H) using whole-mount in situ hybridization at 2 days post fertilization (dpf). Wild-type embryos were derived from an in-cross of laboratory strain AB parents (A and E). *arnt1* mutant embryos were derived from *arnt1;arnt2* heterozygous parents or are maternal zygotic derived from *arnt1* homozygous parents (MZ*arnt1*). *arnt2* mutant embryos were derived from heterozygous parents. *arnt1/2* double homozygous mutant embryos (D and H) were derived from *arnt1;arnt2* double heterozygous parents and identified by cardiovascular phenotype prior to fixation. Panels A'-D' are enlarged images of each embryo's trunk near the end of the yolk extension (area indicated by red box in panels A-D). (A'-D') Black arrows indicate *flk-1* staining in the dorsal longitudinal anastomotic vessels (DLAV), white arrows indicate the dorsal aorta and caudal vein (DA/CV), arrowheads indicate inter-segmental vessels. (E-H) *runx-1* labeling near the end of the yolk extension, arrows indicate blood island region. n=2-5 clutches for each genotype, 10-100 embryos per clutch. All embryos are oriented with anterior to the right and dorsal towards the top. The scale bar in D applies to A-D, the scale bar in D' applies to A'-D', and the scale bar in H applies to E-H. All scale bars are 10 μm.

706

707

708 Figure 3

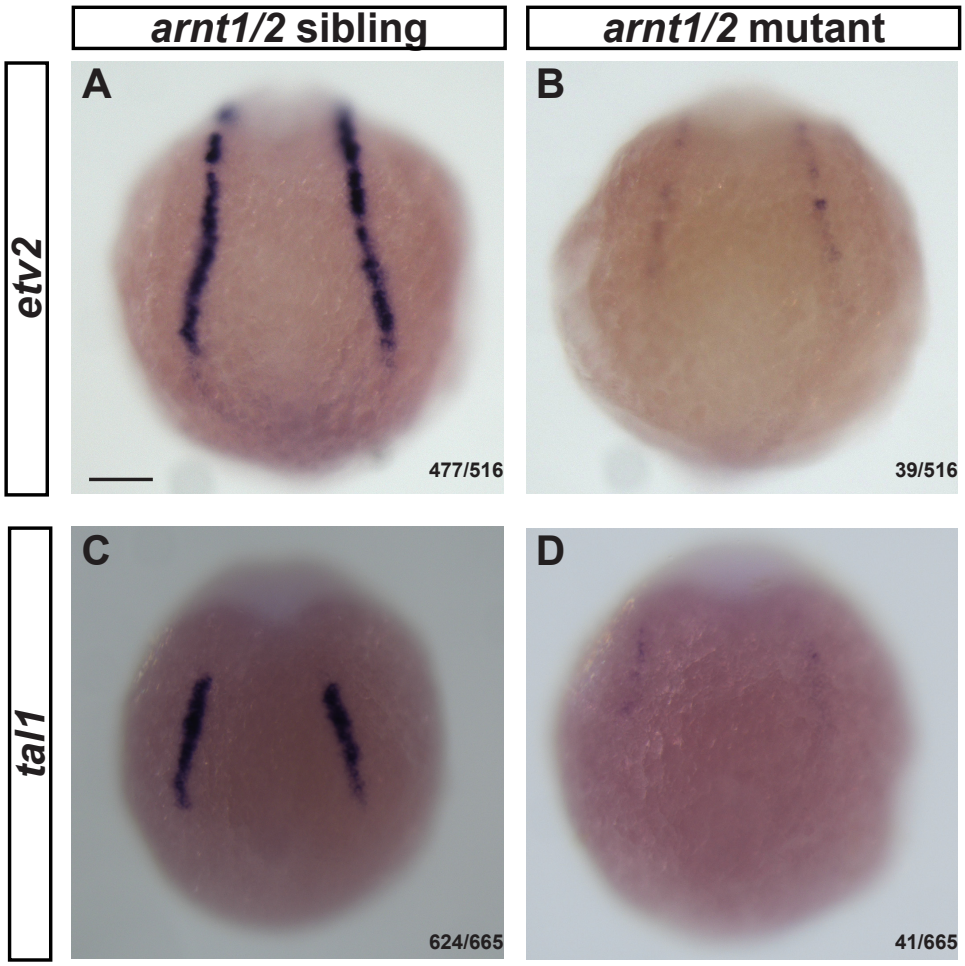

Figure 3. arnt1/2 mutants show decreased etv2 and tal1 expression in the posterior lateral plate mesoderm (PLPM) at 4-6 somite stages. Whole-mount in situ hybridization for *etv2* and *tal1* expression was performed on 4-6 somite stage embryos which were offspring of *arnt1*$^{bcm2/+}$; *arnt2*$^{bcm3/+}$ adult zebrafish. (A) Expression of *etv2* was observed in the PLPM in 92% of embryos (n=477 of 516 total embryos). (B) Limited or no expression of *etv2* was observed in 8% of embryos (n=39 of 516), consistent with the expected Mendelian ratios for *arnt1/2* mutants (6.25%). 24 of the 39 presumptive *arnt1/2* mutants were genotyped and 24/24 embryos were confirmed *arnt1/2* mutants. (C) Expression of *tal1* was observed in 94% of embryos (n=624 of 665 total embryos). (D) Limited or no expression of *tal1* was observed in 6% of embryos (n=41 of 665), consistent with the expected Mendelian ratios for *arnt1/2* mutants (6.25%). 17 of the 41 presumptive *arnt1/2* mutants were genotyped and 14/17 embryos were confirmed *arnt1/2* mutants. All embryos are oriented with dorsal towards the top of the image and posterior is closest to the reader. Scale bar is 10 μm and applies to all images.

709

710

711 Figure 4

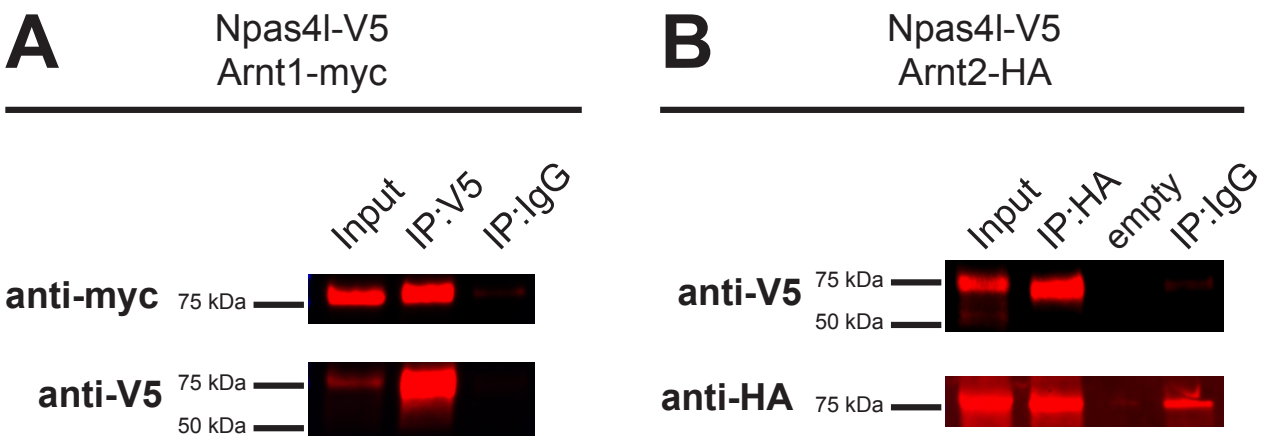

Figure 4. Arnt1 and Arnt2 co-immunoprecipitate with Npas4l. (A) HEK293T cells were transfected with zebrafish Npas4l-V5 and Arnt1-myc. Cells were homogenized (input) and immunoprecipitated (IP) with antibodies aganist V5 or an immunoglobulin G control (IgG). Samples were run on an immunoblot and probed using myc antibodies (anti-myc) to detect the presence of Arnt1-myc (top) or samples were probed using V5 antibodies (anti-V5) to verify sucessful pulldown of Npas4l-V5 (bottom). **(B)** HEK293T cells were transfected with zebrafish Npas4l-V5 and Arnt2-HA. Cells were homogenized and immunoprecipitated with antibodies aganist HA or an IgG control. Samples were run on an immunoblot and probed using V5 antibodies (anti-V5) to detect the presence of Npas4l-V5 (top) or samples were probed using HA antibodies (anti-HA) to verify sucessful pulldown of Arnt2-HA (bottom).

712

713

714

715 Figure 5

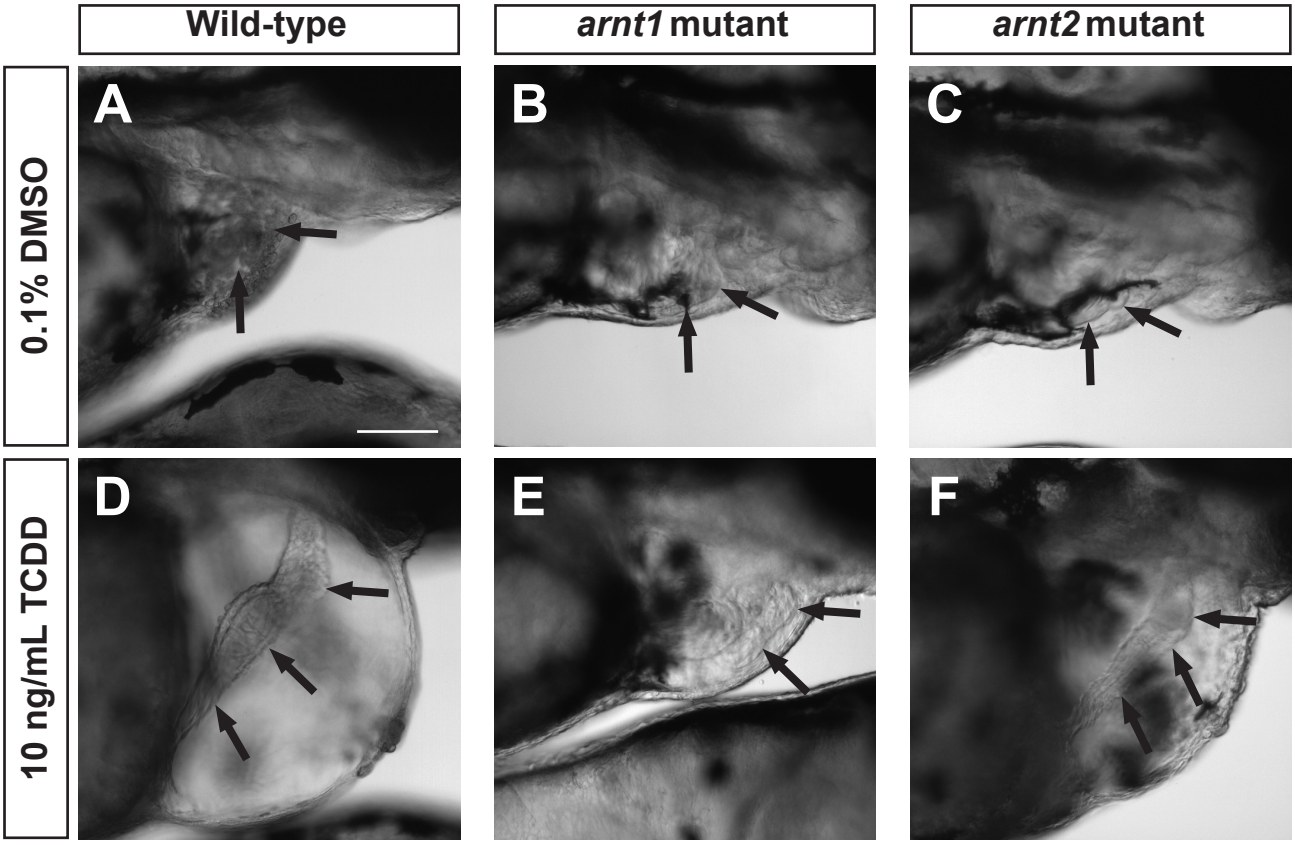

Figure 5. Mutation in *arnt1,* but not *arnt2,* prevents AHR2-dependent TCDD toxicity. Wild type or mutant larvae were exposed to 0.1% DMSO (**A, B, C**), or 2,3,7,8-tetrachlorodibenzodioxin (TCDD) (**D, E, F**) from 1-3 dpf and imaged at 3 dpf. Wildtype embryos exposed to TCDD (**D**) lack an S-shaped cardiac loop and exhibit cardiac edema, unlike their vehicle treated siblings (**A**). *arnt1* homozygous mutant larvae (*arnt1*$^{bcm2/bcm2}$) treated with vehicle and TCDD (**B,E**) show normal heart looping and do not have cardiac edema. *arnt2* homozyous mutant larvae (*arnt1*$^{bcm3/bcm3}$) treated with vehicle (**C**) show expected heart looping similar to wild type siblings, but *arnt2* homozyous mutant larvae treated with TCDD (**F**) lack an S-shaped cardiac loop similar to wild type and exhibit cardiac edema similar to TCDD treated wild-type embryos. Black arrows indicate location of the heart. Embryos were genotyped following imaging and representative images are shown. TCDD treated wildtype siblings of *arnt1* mutant embryos, n= 9 embryos across 3 clutches; TCDD treated *arnt1* mutant larvae, n=21 larvae across 3 clutches. TCDD treated wildtype siblings of *arnt2* larvae, n=19 embryos across 3 cluches; TCDD treated *arnt2* mutant larvae, n=22 embryos across 4 cluches. All embryos are oriented with anterior to the right and dorsal towards the top of the image. Scale bar is 100 µm.

716